

Valley precession in graphene superlattices

S. K. Wang and J. Wang*

Department of Physics, Southeast University, Nanjing 210096, China

(Received 8 June 2015; published 17 August 2015)

One of the challenges in valleytronics is how to effectively manipulate the valley degree of freedom of electrons in graphene. We propose to use a pseudovalley exchange field to rotate the valley, which arises in a graphene superlattice (GS) structure due to the two inequivalent K and K' valleys folded and coupled together. The valley is shown to precess periodically in real space, but the precession itself has a spatial anisotropy unless the GS structure still possesses a rotational symmetry. The pseudovalley exchange field exclusively determines the valley precession periodicity when the electron energy is much larger than the possible GS energy gap. Our findings provide a practical way to control and manipulate the valley degree of freedom in graphene.

DOI: [10.1103/PhysRevB.92.075419](https://doi.org/10.1103/PhysRevB.92.075419)

PACS number(s): 72.80.Vp, 72.10.Bg, 73.43.-f, 85.75.-d

Electrons in two-dimensional (2D) graphenelike materials acquire an extra degree of freedom, i.e., valley, besides the usual charge and spin ones, which comes from the fact that the six corners of the hexagonal Brillouin zone are divided into two inequivalent groups, labeled as the K and K' valleys. Similar to spin, the two valleys are related by the time-reversal symmetry ($K = -K'$) and can be transformed into each other by spatial inversion operation. Due to much momentum difference between the two valleys, the intervalley scattering is severely suppressed [1–4] in clean graphene samples and the valley is largely a conserved quantum number in electron transports. Thus, it is suggested that the valley should be utilized as an information carrier [5–7].

The electronics based on the valley degree of freedom is referred to as valleytronics [5–7] in a similar way that spintronics uses electron spin. Correspondingly, the main challenges in valleytronics should contain the valley generation, detection, and manipulation. Since the valleytronics is still in its infancy, the production and measurement of an imbalance of valley carriers are the principal tasks in this field. Many proposals have been studied to generate valley currents by using graphene nanoribbon [8–10], lattice strain [11–17], electromagnetic field [16–24], optical field [25–27], and line defects [28–30]. As for the valley detection, the usual way is the optical excitation method based on the valley-dependent selection rule [31,32]. Until very recently, Gorbachev *et al.* [33] successfully utilized a purely electric circuit to detect the valley currents via the inverse valley Hall effect [7] in a much similar way to measure spin currents [34,35]. This electric demonstration of valley currents in the experiment will greatly advance the valleytronics [36].

In the valleytronics field, another important and untouched issue is how to manipulate the valley degree of freedom precisely or realize a controllable valley superposed state such as $|\Psi\rangle = \alpha|K\rangle + \beta|K'\rangle$, where $|K\rangle$ and $|K'\rangle$ are the two orthogonal valley basis functions and α and β are the superposed coefficients. This definitely requires a valley exchange field or a valley-dependent interaction correlating the two valleys. A very recent work by Giovannetti *et al.* [37] provides a possible paradigm of such interaction in the graphene-In₂Te₂ superlattice system, where a hexagonal monolayer In₂Te₂ is

deposited on graphene to form a commensurate $\sqrt{3} \times \sqrt{3}$ superlattice, and the coupling between the two valleys, K and K' , was found to open a topological energy gap.

In this work, we show that a pseudovalley exchange field emerges in this graphene-In₂Te₂ superlattice (GS) structure [37], which can precess the valley in real space in a similar way as the Rashba spin-orbit interaction rotates spin in semiconductors [38,39]. It was found that the valley precession is spatially anisotropic depending on the concrete space symmetry of the GS structure, and the precession periodicity is exclusively determined by the pseudovalley exchange field strength when the possible GS energy gap is much smaller than the electron energy. In the following, we will first study the possible valley precession in a lattice model and then address the underlying physical origin based on a continuum model.

The commensurate graphene-In₂Te₂ bilayer [37] is adopted here to study possible valley manipulation. In Fig. 1(a), a schematic GS structure is plotted as well as its hexagonal Brillouin zone, in which the original two valleys, K and K' , of a pristine graphene are folded together. The following lattice model is employed to describe graphene in the GS structure:

$$H = \sum_{\langle ij \rangle} (-t C_i^\dagger C_j + \text{H.c.}) + \sum_{l\delta(\delta=1,2,3)} (\epsilon_{A\delta} C_{lA\delta}^\dagger C_{lA\delta} + \epsilon_{B\delta} C_{lB\delta}^\dagger C_{lB\delta}), \quad (1)$$

where the first term denotes a clean graphene with the hopping energy t between the neighboring carbon atoms, while the second term is the energy modification to graphene from the GS interlayer coupling. $\epsilon_{A(B)\delta}$ represents the corresponding on-site energy of the six A and B carbon atoms in a supercell marked in Fig. 1(a), and it can, in principle, be changed by an electric field or a strain field when the GS is grown on a suitable substrate. Here we neglect the possible modification to the hopping energy t since it is largely a second-order energy correction [40,41] much smaller than $\epsilon_{A(B)\delta}$.

To study the valley precession, we consider a G/GS/G transport model, schematically shown in Fig. 1(b), where the GS is only assumed in the middle region. The two K and K' valleys are still independent in the left and right pristine G regions. By assuming that a τ -valley ($\tau = K, K'$) electron from the left G region tunnels through the GS layer, one can calculate the τ' -valley ($\tau' = K, K'$) probability in the right G region. According to the standard nonequilibrium Green's

*jwang@seu.edu.cn

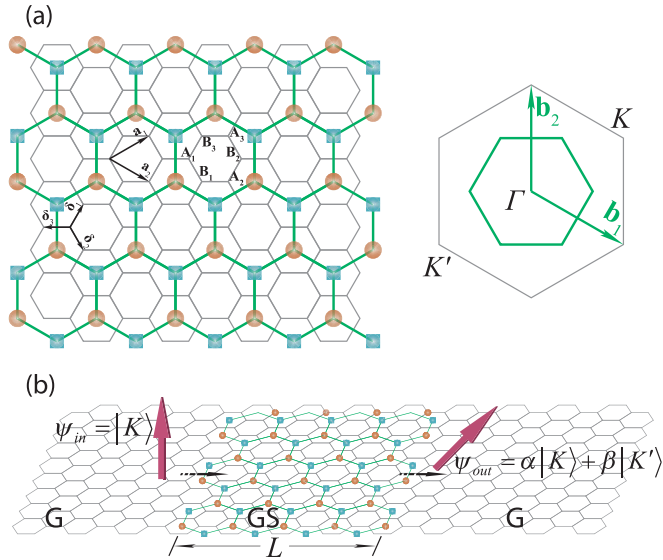


FIG. 1. (Color online) (a) Schematic of a commensurate graphene superlattice composed of a single-layer graphene and a In_2Te_2 monolayer. The GS has a $\sqrt{3}\mathbf{a}_1 \times \sqrt{3}\mathbf{a}_2$ supercell with a contracted hexagonal Brillouin zone (right panel) and the original K and K' are folded together at the Γ point. (b) A two-terminal G/GS/G device of the valley transport. A K -valley wave function $\psi_{\text{in}} = |K\rangle$ incident from the left G region is transformed into a valley superposed state in the right G region, $\psi_{\text{out}} = \alpha|K\rangle + \beta|K'\rangle$. L is the GS layer length.

function method, the transmission is given by

$$T_{x(y)}^{\tau\tau'} = \text{Tr}[\Gamma_L^\tau G^r \Gamma_R^{\tau'} G^a], \quad (2)$$

where $G^{r(a)}$ is the retarded (advanced) Green's function of the GS structure, $\Gamma_{L(R)}^\tau$ is the τ -valley linewidth matrix of the left (right) G region, and the trace is over the transverse modes (or transverse momenta, as the system has transverse translational symmetry [42]). Since the different valleys (K or K') represent different momenta, the valley transport may rely on its propagating direction in real space. Two typical transport directions are considered: one is along the armchair edge of graphene labeled as the x direction, and the other is along the zigzag edge labeled as the y direction.

For simplicity, we focus on the 1D transport case by considering a zero transverse momentum [42,43] in the above transmission formula. In Fig. 2, the transmission coefficients are plotted as a function of the GS length L/a (a is the graphene lattice constant). In numerics, the hopping energy t is set as an energy unit and the temperature is set as zero. It is clearly shown that the valley-conserved transmission ($T_{x(y)}^{KK}$) and valley-flip transmission ($T_{x(y)}^{KK'}$) exhibit a perfect oscillation, and $T_{x(y)}^{KK} + T_{x(y)}^{KK'} = 1$. This indicates that a valley-dependent interaction in the GS region can precess valley and lead to a valley superposed state in the right G region when a K electron is incident from the left G region. Nevertheless, the valley precession is spatially anisotropic because the periodicity of T_x along the x direction [Figs. 2(a) and 2(c)] is clearly different from that of T_y along the y direction [Figs. 2(b) and 2(d)].

In Figs. 2(c) and 2(d), we showed that the transmissions keep nearly unchanged when the energy of incident electrons

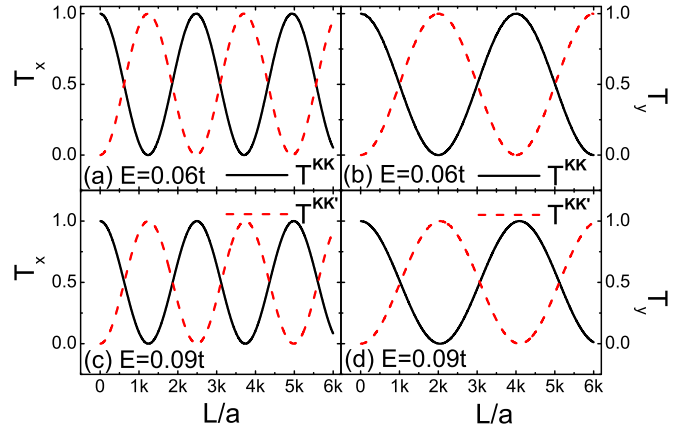


FIG. 2. (Color online) Valley-dependent transmission $T_{x(y)}^{KK(K')}$ as a function of the GS layer length L . $\epsilon_{A1} = 0.006t$, $\epsilon_{B1} = \epsilon_{A1}/4$, and other site energy $\epsilon_{A(B)\delta \neq 1} = 0$. Different electron energies are marked in each panel.

E is varied. So it is expected that the interlayer coupling strength in the GS represented by $\epsilon_{A(B)\delta}$ should play a decisive role in determining the valley precession. In Fig. 3, we plotted the transmissions as a function of the site energy ϵ_{A1} . The results agree with those in Fig. 2: valley can be modulated periodically and the precession periodicity is spatially anisotropic. Meanwhile, the precession periodicity is also sensitive to the spatial configuration of $\epsilon_{A(B)\delta}$ in a GS supercell by comparing the upper and lower panels in Fig. 3. Note that the K' -valley transmission $T_{x(y)}^{K'(K)}$ (not shown) has the same behaviors as those in Figs. 2 and 3 due to the G/GS/G model preserving time-reversal symmetry and left-right inversion symmetry, $T_{x(y)}^{\tau\tau'} = T_{x(y)}^{\bar{\tau}\bar{\tau}'}$ with $\bar{\tau} = -\tau$.

To interpret the above numerical results, one needs first to transform the lattice-version Hamiltonian into a Bloch-representation one, and then derives a low-energy effective Hamiltonian by taking the GS interlayer's coupling as a perturbation [40,41],

$$H_e = \hbar v_f(k_x \sigma_x + k_y \sigma_y \tau_z) + \epsilon_0 + \tilde{B}_0 \tau_0 + \tilde{B}_x \tau_x + \tilde{B}_y \tau_y, \quad (3)$$

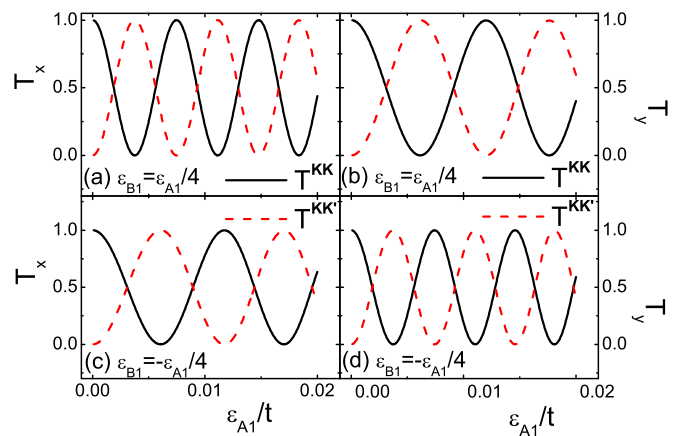


FIG. 3. (Color online) Valley-dependent transmission $T_{x(y)}^{KK(K')}$ as a function of the site energy ϵ_{A1} . $\epsilon_{B1} = \pm\epsilon_{A1}/4$ marked in panels with $\epsilon_{A(B)\delta \neq 1} = 0$, the length of the GS region $L/a = 2000$, and electron energy $E = 0.06t$.

where $\hbar v_f = \sqrt{3}at/2$, σ represents the lattice pseudospin Pauli matrix, τ is the valley Pauli matrix, τ_0 is a unit matrix, and $k_{x(y)}$ is the electron momentum. The first term is the usual low-energy massless Dirac equation of graphene, while the remainder come from the site-energy modification $\epsilon_{A(B)\delta}$, $\epsilon_0 = \frac{1}{6} \sum_{\delta} (\epsilon_{A\delta} + \epsilon_{B\delta})$ is a constant potential, $\tilde{B}_0 = \frac{1}{6} \sum_{\delta} (\epsilon_{A\delta} - \epsilon_{B\delta}) \sigma_z$, $\tilde{B}_x = \frac{1}{6} [(\tilde{a} + \tilde{b})\sigma_0 + (\tilde{a} - \tilde{b})\sigma_z]$ with $\tilde{a}(\tilde{b}) = [\epsilon_{A(B)1} - \frac{\epsilon_{A(B)2}}{2} - \frac{\epsilon_{A(B)3}}{2}]$, and $\tilde{B}_y = \frac{1}{6} [(\tilde{c} + \tilde{d})\sigma_0 + (\tilde{c} - \tilde{d})\sigma_z]$ with $\tilde{c}(\tilde{d}) = \frac{\sqrt{3}}{2} [\epsilon_{A(B)2} - \epsilon_{A(B)3}]$. Since $\tilde{B}_i (i = x, y)$ comes from the site-energy modifications in a GS supercell, it stands for a complicated lattice pseudospin. A nonzero lattice pseudospin in graphene shall be closely related to a valley imbalance, i.e., the $\tilde{\mathbf{B}}$ field is equivalent to a kind of nonzero τ_z field so that the coupling $\tilde{B}_x \tau_x + \tilde{B}_y \tau_y$ can be referred to as a pseudovalley exchange interaction. It is noted that the $\tilde{\mathbf{B}}$ field here still fulfills the time-reversal symmetry.

Based on the above effective Hamiltonian, we can solve the valley-dependent transmission $T_{x(y)}^{\tau\tau'}$ in the transport model of Fig. 1(b). Only for several special $\epsilon_{A(B)\delta}$ configurations are the analytic results available, in which the GS shall have a certain space symmetry. We first consider a simple case that only one carbon atom in the supercell has a nonzero site-energy modification, $\epsilon_{A1} \neq 0$, and others vanishing. The H_e eigenvalues are given by $E_1^{\pm} = \pm \hbar v_f \sqrt{k_x^2 + k_y^2}$ and $E_2^{\pm} = \pm \sqrt{\hbar^2 v_f^2 (k_x^2 + k_y^2) + \Delta^2} \pm \Delta$, where $\Delta = \epsilon_{A1}/3$ is the energy gap for E_2^{\pm} and can also stand for the pseudovalley exchange field strength, $\tilde{B}_x = \Delta(\sigma_0 + \sigma_z)/2$. By considering an incident K -valley wave function $\psi_{\text{in}} = |K\rangle$ and the outgoing wave function $\psi_{\text{out}} = \alpha|K\rangle + \beta|K'\rangle$ in the G/GS/G model, one can directly obtain the transmission amplitudes by using a quantum scattering method,

$$\begin{aligned} \alpha &= \frac{-e^{ik_1 - ik_2}(\chi + 1)^2 + e^{ik_1 + ik_2}(\chi - 1)^2 - 4}{2e^{ik_1 + ik_2}(\chi - 1)^2 - 2e^{ik_1 - ik_2}(\chi + 1)^2}, \\ \beta &= \frac{e^{ik_1 - ik_2}(\chi + 1)^2 - e^{ik_1 + ik_2}(\chi - 1)^2 - 4}{2e^{ik_1 + ik_2}(\chi - 1)^2 - 2e^{ik_1 - ik_2}(\chi + 1)^2}, \end{aligned} \quad (4)$$

where $\chi = \sqrt{E/(E - 2\Delta)}$, $k_1 = LE/\hbar v_f$, $k_2 = L\sqrt{E(E - 2\Delta)}/\hbar v_f$, and E is the electron energy conserved in the scattering event. When $E \gg \Delta$, $\chi \simeq 1$ and the transmission coefficients approximate

$$\begin{aligned} T^{KK} &= |\alpha|^2 \simeq \cos^2 \kappa_1 L, \\ T^{KK'} &= |\beta|^2 \simeq \sin^2 \kappa_1 L, \end{aligned} \quad (5)$$

with $\kappa_1 = \Delta/2\hbar v_f$, i.e., the transmission is independent of energy E , the K -valley incident from the left G region is perfectly rotated by the pseudovalley exchange field \tilde{B}_x in the GS region, and the precession periodicity is solely determined by Δ , the \tilde{B}_x field strength. From this point, the pseudovalley exchange field $\tilde{\mathbf{B}}$ resembles the Rashba spin-orbit interaction [38] in semiconductors, which is well known to preserve time-reversal symmetry and determine exclusively spin precession in the spin field-effect transistor [39]. But the difference between them is also clear: the $\tilde{\mathbf{B}}$ field here may open an insulating gap ($\sim \Delta$) and the system enters a new quantum phase, i.e., the valley quantum Hall insulator [7,37]. Therefore, the valley precession is prohibited when the electron energy is in the gap

of the GS, and it will be energy dependent when the energy E is near the band edge. For instance, when $E = 2\Delta$, $\alpha = \beta = 1/2$ and $T^{KK} + T^{KK'} = 1/2$, whereas $T^{KK} + T^{KK'} = 1$ only when $E \gg \Delta$, and the valley precession is perfect. From eigenvalues of H_e , the k_x and k_y is symmetric and so the valley precession is spatially isotropic. This stems from the fact that the GS structure with a single-atom modification $\epsilon_{A1} \neq 0$ has a rotational symmetry C_{3v} , although it is already lower than the original C_{6v} symmetry of a pristine graphene.

We further consider a reduced lattice symmetry of the GS structure by setting $\epsilon_{A1} = \epsilon_{B1} \neq 0$ and $\epsilon_{A(B)\delta \neq 1} = 0$. The eigenvalues of the GS are obtained as $E = \Delta \pm \hbar v_f \sqrt{(k_x \pm \kappa_2)^2 + k_y^2}$ with $\kappa_2 = 2\kappa_1$. Here the momenta k_x and k_y are no longer symmetric, and electrons meet a barrier of the height Δ along the y axis and null along the x axis. The transmission coefficients along the x axis are given by

$$\begin{aligned} T_x^{KK} &= \left| \frac{e^{ik_1} + e^{ik'_2}}{2e^{ik_1}} \right|^2 = \cos^2 \kappa_2 L, \\ T_x^{KK'} &= \left| \frac{e^{ik_1} - e^{ik'_2}}{2e^{ik_1}} \right|^2 = \sin^2 \kappa_2 L, \end{aligned} \quad (6)$$

with $k'_2 = L(E - 2\Delta)/\hbar v_f$. Here the transmission results are rigorous without any approximation because there is no energy gap along the x axis, the valley exhibits a perfect oscillation, and the \tilde{B}_x strength ($\tilde{B}_x = \Delta\sigma_0$) solely determines the valley precession without limitation on E . Along the y axis, there is almost no valley modulation, $T_y^{KK} = 1$ and $T_y^{KK'} = 0$ when $E \gg \Delta$. From the H_e eigenfunctions (chiral-valley eigenfunctions due to \tilde{B}_x in the GS) propagating along the y axis, the two wave functions share a same wave vector for a fixed E , so there is no dynamic phase difference leading to the valley precession.

For the case of nonzero $\epsilon_{A1} = \epsilon_{B1}$ above, the valley can be beautifully rotated along the x axis and keeps almost intact along the y axis. This is closely related to the lattice symmetry again. The GS structure has a reduced C_{2v} symmetry with the mirror operation plane perpendicular to the y axis, and the operators are given by [44] $M_y^+ k_y M_y = -k_y$, $M_y^+ k_x M_y = k_x$, $M_y^+ \sigma_y(\tau_y) M_y = \sigma_y(\tau_y)$, $M_y^+ \sigma_{x(z)}(\tau_{x(z)}) M_y = -\sigma_{x(z)}(\tau_{x(z)})$, and $C_2^+ k_{x(y)} C_2 = e^{i\pi} k_{x(y)}$. The pseudovalley exchange field term $\tilde{\mathbf{B}} \cdot \boldsymbol{\tau}$ keeps unchanged under M_y operation. The GS structure acts as a pristine graphene upon the y axis, so the K and K' valleys are not coupled together effectively. Oppositely, $M_x^+ \tilde{\mathbf{B}} \cdot \boldsymbol{\tau} M_x \neq \tilde{\mathbf{B}} \cdot \boldsymbol{\tau}$, the two valleys, K and K' , can couple to each other along the x axis, so the valley precession is feasible. As a matter of fact, there is another extreme case of the GS structure: $\epsilon_{A1} = -\epsilon_{B1} \neq 0$ with $\epsilon_{A(B)\delta \neq 1} = 0$, and the mirror symmetry plane is changed to be perpendicular to the x axis. Within the same method, the valley transmission amplitudes along the y axis are given by

$$\begin{aligned} \alpha &= \sum_{j(j=+,-)} \frac{2\chi_j e^{-ik_1}}{e^{ik_{yj}}(\chi_j - 1)^2 + e^{-ik_{yj}}(\chi_j + 1)^2}, \\ \beta &= \sum_{j(j=+,-)} \frac{2j\chi_j e^{-ik_1}}{e^{ik_{yj}}(\chi_j - 1)^2 + e^{-ik_{yj}}(\chi_j + 1)^2}, \end{aligned} \quad (7)$$

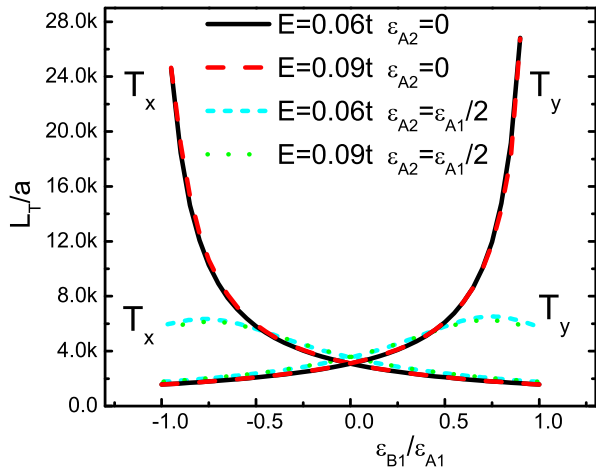


FIG. 4. (Color online) Periodicity of the transmission T_x and T_y as a function of $\epsilon_{B1}/\epsilon_{A1}$. Different site energy ϵ_{A2} and electron energy E are marked in the panel; $\epsilon_{A1} = 0.006t$ and other site energy $\epsilon_{A(B)\delta} = 0$.

with $k_{y\pm} = L\sqrt{(E \pm \Delta)^2 - \Delta^2}/\hbar v_f$, $\chi_+ = \sqrt{(E + 2\Delta)/E}$, and $\chi_- = \sqrt{E/(E - 2\Delta)}$. When $E \gg \Delta$, we can obtain the same transmission coefficients of Eq. (6), $T_y^{KK} = \cos^2 \kappa_2 L$ and $T_y^{KK'} = \sin^2 \kappa_2 L$, and, moreover, $T_x^{KK} = 1$ and $T_x^{KK'} = 0$. Here the valley precession also exhibits extremely spatial anisotropy, since the mirror plane is perpendicular to the x axis and the two valleys can be transformed into each other without effective coupling. Hence, the valley modulation can only be carried out along the y direction for this $\epsilon_{A1} = -\epsilon_{B1} \neq 0$ case.

For a general $\epsilon_{AB\delta}$ configuration (\vec{B} field) in the GS, there is no mirror symmetry plane and the valley modulation in any direction is possible. Nevertheless, the spatial anisotropy still exists, as shown in Fig. 3, unless the GS structure has a rotational symmetry like C_{3v} , as we discussed earlier. The space anisotropy of valley precession can be understood as follows: for one thing, the valleys are from the corners of the hexagonal Brillouin zone with different wave vectors, so the dynamic-phase accumulations of different valley electrons moving in the GS media are different; for another, the pseudovalue exchange field \vec{B} is explicitly determined by the spatial configuration of $\epsilon_{AB\delta}$ in a GS supercell. These two factors together lead to valley precession dramatically relying on the propagation direction of electrons.

The analytical valley precession is not obtainable for a general \vec{B} field and, instead, we present numerical results of the precession periodicity in Fig. 4 based on the lattice model above. The valley precession periodicity L_T for T_x and T_y is plotted as a function of $\epsilon_{B1}/\epsilon_{A1}$ with and without ϵ_{A2} . The three analytical results discussed above [Eqs. (5)–(7)] are

also included in the figure, as denoted by solid and dashed lines: at $\epsilon_{A1} = \epsilon_{B1}$, valleys cannot be modulated along the y axis and L_T is divergent; at $\epsilon_{A1} = -\epsilon_{B1}$, the valley cannot be rotated along the x axis; and at $\epsilon_{B1} = 0$, the valley precession is spatially isotropic. When any other site energy $\epsilon_{A(B)\delta \neq 1}$ is introduced or combined together, L_T shows no divergence and changes slightly with variation of $\epsilon_{B1}/\epsilon_{A1}$, as denoted by the dotted and short dashed lines in Fig. 4. Thus, the more the GS lattice approaches to a rotational symmetry, the more homogenous the valley precession becomes. It is shown again that the valley precession periodicity L_T is nearly independent of the electron energy E when $E \gg \epsilon_{A(B)\delta}$.

From the above discussions, the key point for precessing valley is the GS structure, which couples the original valleys, K and K' , and leads to a pseudovalue exchange field \vec{B} . Note that this \vec{B} field can be used not only to implement a valley superposed state such as $\alpha|K\rangle + \beta|K'\rangle$, but also to control the relative phase between α and β by varying the \vec{B} field direction. This can be seen from the Hamiltonian [Eq. (3)] of the GS system; the relative magnitudes of B_x and B_y will account for the phase of the valley superposed state of the GS structure. Theoretically, as long as a graphene superlattice not limited to tripled enlargement would fold the K and K' valleys into a same point in the reciprocal lattice space, it may be used to control valley. The commensurate graphene/h-BN heterostructure [45] with a huge supercell is a good demonstration. Due to the successful measurement of the inverse valley Hall effect in experiment [33], which transforms valley currents into a measurable electric voltage/current signal, one can use a GS structure to rotate the input valley direction so as to affect the measured voltage/current. Moreover, the interlayer coupling in our GS model is conveniently modulated by an electric field or a strain field when the GS grows in a controllable substrate.

In summary, we have investigated the possible valley precession in the graphene-In₂Te₂ superlattice structure based on a transport model. Both numerics and analysis showed that the pseudovalue exchange field born in the GS structure can be used to manipulate electron valley effectively, resembling the Rashba spin-orbit interaction rotating spin. The valley precession was shown to exhibit a spatial anisotropy and crucially depend on the GS lattice symmetry. The precession periodicity is solely determined by the pseudovalue exchange field when the electron energy is much larger than the possible GS energy gap. Our findings may shed light on manipulating the valley degree of freedom of graphene in a nonmagnetic way.

The work is supported by the Natural Science Foundation of China (Grant No. 11274059) and the Natural Science Foundation of Jiangsu Province (Grant No. BK20131284). J.W. is also thankful for support from the Fundamental Research Funds for the Central Universities.

- [1] A. F. Morpurgo and F. Guinea, *Phys. Rev. Lett.* **97**, 196804 (2006).
 [2] S. V. Morozov, K. S. Novoselov, M. I. Katsnelson, F. Schedin, L. A. Ponomarenko, D. Jiang, and A. K. Geim, *Phys. Rev. Lett.* **97**, 016801 (2006).

- [3] R. V. Gorbachev, F. V. Tikhonenko, A. S. Mayorov, D. W. Horsell, and A. K. Savchenko, *Phys. Rev. Lett.* **98**, 176805 (2007).
 [4] J.-H. Chen, W. G. Cullen, C. Jang, M. S. Fuhrer, and E. D. Williams, *Phys. Rev. Lett.* **102**, 236805 (2009).

- [5] D. Pesin and A. H. MacDonald, *Nat. Mater.* **11**, 409 (2012).
- [6] K. Behnia, *Nat. Nanotech.* **7**, 488 (2012).
- [7] D. Xiao, W. Yao, and Q. Niu, *Phys. Rev. Lett.* **99**, 236809 (2007).
- [8] A. Rycerz, J. Tworzydło, and C. W. J. Beenakker, *Nat. Phys.* **3**, 172 (2007).
- [9] A. R. Akhmerov, J. H. Bardarson, A. Rycerz, and C. W. J. Beenakker, *Phys. Rev. B* **77**, 205416 (2008).
- [10] H. Schomerus, *Phys. Rev. B* **82**, 165409 (2010).
- [11] F. Zhai and K. Chang, *Phys. Rev. B* **85**, 155415 (2012).
- [12] Z.-Z. Cao, Y.-F. Cheng, and G.-Q. Li, *Appl. Phys. Lett.* **101**, 253507 (2012).
- [13] T. Fujita, M. B. A. Jalil, and S. G. Tan, *Appl. Phys. Lett.* **97**, 043508 (2010).
- [14] T. Low and F. Guinea, *Nano Lett.* **10**, 3551 (2010).
- [15] Z. Khatibi, H. Rostami, and R. Asgari, *Phys. Rev. B* **88**, 195426 (2013).
- [16] Z. Wu, F. Zhai, F. M. Peeters, H. Q. Xu, and K. Chang, *Phys. Rev. Lett.* **106**, 176802 (2011).
- [17] Y. Jiang, T. Low, K. Chang, M. I. Katsnelson, and F. Guinea, *Phys. Rev. Lett.* **110**, 046601 (2013).
- [18] L. E. Golub, S. A. Tarasenko, M. V. Entin, and L. I. Magarill, *Phys. Rev. B* **84**, 195408 (2011).
- [19] G. Y. Wu, N.-Y. Lue, and Y.-C. Chen, *Phys. Rev. B* **88**, 125422 (2013).
- [20] J. Wang, K. S. Chan, and Zijing Lin, *Appl. Phys. Lett.* **104**, 013105 (2014).
- [21] S. K. Wang, J. Wang, and K. S. Chan, *New J. Phys.* **16**, 045015 (2014).
- [22] A. Chaves, L. Covaci, Kh. Yu. Rakhimov, G. A. Farias, and F. M. Peeters, *Phys. Rev. B* **82**, 205430 (2010).
- [23] J. Wang and S. Fischer, *Phys. Rev. B* **89**, 245421 (2014).
- [24] M. M. Grujić, M. Ž. Tadić, and F. M. Peeters, *Phys. Rev. Lett.* **113**, 046601 (2014).
- [25] M. Ezawa, *Phys. Rev. Lett.* **110**, 026603 (2013).
- [26] H. L. Zeng, J. F. Dai, W. Yao, D. Xiao, and X. D. Cui, *Nat. Nanotech.* **7**, 490 (2012).
- [27] W. Yao, D. Xiao, and Q. Niu, *Phys. Rev. B* **77**, 235406 (2008).
- [28] D. Gunlycke and C. T. White, *Phys. Rev. Lett.* **106**, 136806 (2011).
- [29] Y. Liu, J.-T. Song, Y.-X. Li, Y. Liu, and Q.-F. Sun, *Phys. Rev. B* **87**, 195445 (2013).
- [30] J.-H. Chen, G. Autès, N. Alem, F. Gargiulo, A. Gautam, M. Linck, C. Kisielowski, O. V. Yazyev, S. G. Louie, and A. Zettl, *Phys. Rev. B* **89**, 121407(R) (2014).
- [31] T. Cao, G. Wang, W. Han, H. Ye, Ch. Zhu, J. Shi, Q. Niu, P. Tan, E. Wang, B. Liu, and J. Feng, *Nat. Commun.* **3**, 887 (2012).
- [32] K. F. Mak, K. He, J. Shan, and T. F. Heinz, *Nat. Nanotechnol.* **7**, 494 (2012).
- [33] R. V. Gorbachev, J. C. W. Song, G. L. Yu, A. V. Kretinin, F. Withers, Y. Cao, A. Mishchenko, I. V. Grigorieva, K. S. Novoselov, L. S. Levitov, and A. K. Geim, *Science* **346**, 448 (2014).
- [34] S. O. Valenzuela and M. Tinkham, *Nature (London)* **442**, 176 (2006).
- [35] T. Kimura, Y. Otani, T. Sato, S. Takahashi, and S. Maekawa, *Phys. Rev. Lett.* **98**, 156601 (2007).
- [36] M. B. Lundeberg and J. A. Folk, *Science* **346**, 422 (2014).
- [37] G. Giovannetti, M. Capone, J. van den Brink, and C. Ortix, *Phys. Rev. B* **91**, 121417(R) (2015).
- [38] Y. A. Bychkov and E. I. Rashba, *J. Phys. C* **17**, 6039 (1984).
- [39] S. Datta and B. Das, *Appl. Phys. Lett.* **56**, 665 (1990).
- [40] A. Pachoud, A. Ferreira, B. Özyilmaz, and A. H. Castro Neto, *Phys. Rev. B* **90**, 035444 (2014).
- [41] Y. F. Ren, X. Z. Deng, C. S. Li, J. Jung, C. G. Zeng, Z. Y. Zhang, Q. Niu, and Z. H. Qiao, *Phys. Rev. B* **91**, 245415 (2015).
- [42] J. Wang, Y. H. Yang, and K. S. Chan, *Phys. Rev. B* **89**, 064501 (2014).
- [43] P. Burset, A. Levy Yeyati, and A. Martín-Rodero, *Phys. Rev. B* **77**, 205425 (2008).
- [44] H. Zhang, K. S. Chan, Z. Lin, and J. Wang, *Phys. Rev. B* **85**, 024501 (2012).
- [45] J. C. W. Song, P. Samutpraphoot, and L. S. Levitov, *arXiv:1404.4019*.